Journal of Neuroscience Research

Journal of Neuroscience Research 93:1009–1018 (2015)

Brain Energy Metabolism Measured by ^{13}C Magnetic Resonance Spectroscopy In Vivo Upon Infusion of [3-^{13}C]Lactate

João M.N. Duarte,[1]* Freya-Merret Girault,[1] and Rolf Gruetter[1,2,3]

[1]Laboratory for Functional and Metabolic Imaging, École Polytechnique Fédérale de Lausanne, Lausanne, Switzerland
[2]Department of Radiology, University of Lausanne, Lausanne, Switzerland
[3]Department of Radiology, University of Geneva, Geneva, Switzerland

The brain uses lactate produced by glycolysis as an energy source. How lactate originated from the blood stream is used to fuel brain metabolism is not clear. The current study measures brain metabolic fluxes and estimates the amount of pyruvate that becomes labeled in glial and neuronal compartments upon infusion of [3-^{13}C]lactate. For that, labeling incorporation into carbons of glutamate and glutamine was measured by ^{13}C magnetic resonance spectroscopy at 14.1 T and analyzed with a two-compartment model of brain metabolism to estimate rates of mitochondrial oxidation, glial pyruvate carboxylation, and the glutamate–glutamine cycle as well as pyruvate fractional enrichments. Extracerebral lactate at supraphysiological levels contributes at least two-fold more to replenish the neuronal than the glial pyruvate pools. The rates of mitochondrial oxidation in neurons and glia, pyruvate carboxylase, and glutamate–glutamine cycles were similar to those estimated by administration of ^{13}C-enriched glucose, the main fuel of brain energy metabolism. These results are in agreement with primary utilization of exogenous lactate in neurons rather than astrocytes.

Key words: lactate; ^{13}C MRS; brain; metabolism

Although brain function depends on an adequate supply of oxygen and glucose, brain energy requirements can be fulfilled by oxidation of alternative substrates, such as lactate (Dienel, 2012a). Lactate acts as a buffer between glycolysis and mitochondrial oxidative metabolism, functions as a regulator of cellular redox state by conversion to pyruvate, and is exchanged as a fuel between cells and tissues, depending on relative glycolytic and oxidative rates (Brooks, 2009). Although the brain exports lactate at rest, a net flux of lactate into the brain occurs at elevated blood lactate levels (Gallagher et al., 2009; Rasmussen et al., 2010; van Hall, 2010). Exogenous lactate is not a necessary brain fuel in vivo, so cellular utilization of lactate in the brain has been a matter of debate (Dienel, 2012b; Hertz, 2012). Lactate is generated and oxidized by both neurons and astrocytes, but the magnitude and direction of cell-to-cell lactate shuttling coupled to its oxidation and/or release from the brain remains to be firmly established. Two decades ago, Pellerin and Magistretti (1994) proposed an astrocyte–neuron lactate shuttle in which glutamate released into the synaptic cleft during synaptic activity is cotransported with Na^+ into astrocytes, leading to stimulation of the Na^+/K^+ ATPase that, in turn, results in stimulation of the glycolytic flux and increased glucose uptake from surrounding capillaries. The end product of glycolysis, lactate, is then exported by astrocytes and taken up by neurons, where it can be oxidized in mitochondria for ATP synthesis (Pellerin and Magistretti, 1994). Recently, evidence in vivo has confirmed the requirement of astrocyte-derived lactate to sustain brain functions. In particular, lactate produced by astrocytes from either glucose or glycogen stores is involved in memory processes (Newman et al., 2011; Suzuki et al., 2011) and can be used as fuel for axonal function (Wender et al., 2000) and for myelin synthesis in oligodendroglia (Rinholm et al., 2011; Lee et al., 2012). Because the end-feet of astrocytes ensheath blood vessels, it is plausible that blood-borne lactate is redirected from astrocytes to neurons and oligodendrocytes for further oxidation.

Lactate administration is neuroprotective against brain damage upon limited glucose and/or oxygen availability (Schurr et al., 1997, 2001), traumatic brain injury (Cureton et al., 2010), and glutamate excitotoxicity (Schurr et al., 1999; Ros et al., 2001; Berthet et al., 2009). Because lactate requires oxygen for its metabolism, and excitotoxicity increases lactate while reducing glucose levels, effects of exogenous lactate in sparing brain glucose

Contract grant sponsor: Swiss National Science Foundation; Contract grant numbers: 131087 (to R.G.); 148250 (to J.M.N.D.); Contract grant sponsor: Centre d'Imagerie BioMédicale of the UNIL, UNIGE, HUG, CHUV, EPFL, and the Leenaards and Jeantet Foundations.

*Correspondence to: João M. N. Duarte, EPFL SB IPMC LIFMET, Station 6 (Bâtiment CH), CH-1015 Lausanne, Switzerland.
E-mail: joao.duarte@epfl.ch

Received 15 September 2014; Revised 6 November 2014; Accepted 10 November 2014

Published online 17 December 2014 in Wiley Online Library (wileyonlinelibrary.com). DOI: 10.1002/jnr.23531

and reducing the extension of lesions may be related to its intracellular signaling roles rather than to its role as a fuel. In particular, lactate acts as a transmitter of metabolic information by modulating prostaglandin action and cerebral vasodilatation causing cerebral blood flow to increase, regulates the $NADH/NAD^+$ redox ratio by conversion to pyruvate, and activates the G-protein-coupled receptor GPR81 (also known as *hydroxycarboxylic acid receptor 1*) in neurons, astrocytes, and capillaries, inhibiting cAMP production (Gordon et al., 2008; Bergersen and Gjedde, 2012; Lauritzen et al., 2014). Thus, lactate physiologically produced by astrocytes may also function as a signaling molecule.

Magnetic resonance spectroscopy (MRS) studies have revealed similar peak patterns in ^{13}C spectra after infusion of ^{13}C-enriched glucose and lactate, contrasting with spectra obtained after infusing ^{13}C-acetate that is specifically oxidized in glial cells (Boumezbeur et al., 2010). Metabolic studies in vivo using ^{13}C MRS allow the noninvasive quantification of fluxes through biochemical pathways of oxidative metabolism in both neurons and astrocytes (Lanz et al., 2013). Mathematical modeling of ^{13}C MRS data can be employed to estimate further the relative contribution of ^{13}C-enriched substrates to mitochondrial oxidation within the neuronal and astrocytic compartments (Jeffrey et al., 2013). Therefore, the current study tests the hypothesis that exogenously provided [3-^{13}C]lactate is preferentially oxidized in neurons rather than glial cells, leading to differential fractional enrichment (FE) of the pyruvate pools, by using ^{13}C MRS in vivo in the rat brain.

MATERIALS AND METHODS

Chemicals

Sodium [3-^{13}C]lactate (45–55% w/w), ^2HCl (20% w/w), NaO^2H (40% w/w) and ^2H_2O were purchased from Sigma-Aldrich (Basel, Switzerland); isoflurane was purchased from Nicholas Piramal India (London, United Kingdom); and α-chloralose was purchased from Acros Organics (Geel, Belgium). All other chemicals were of the purest grade available from either Sigma-Aldrich or Merck (Darmstadt, Germany).

Animals

All experimental procedures involving animals were approved by the local ethics committee (EXPANIM-SCAV, Switzerland). Male Sprague-Dawley rats (256 ± 8 g, n = 8; purchased from Charles River Laboratories) were briefly anesthetized with 4% isoflurane in air and then were intubated and mechanically ventilated with a mixture of 30% O_2 in air by using a pressure-driven ventilator (MRI-1; CWE, Ardmore, PA). Witgh animals under 2% isoflurane anesthesia, catheters were placed into a femoral artery and a femoral vein as previously described (Duarte et al., 2009). The artery was used for blood sampling and for continuous monitoring of blood pressure and heart rate with the SA Instruments (Stony Brook, NY) animal monitoring system. The vein was used as an administration route for phosphate-buffered saline (PBS) solutions (in mM: 2.7 KCl, 8.1 Na_2HPO_4, 1.5 KH_2PO_4, 137 NaCl) containing α-chloralose (5 mg/ml, pH 7), [3-^{13}C]lactate (0.9 M, pH 5), or glucose (1.1 M, pH 7).

After surgery, anesthesia was achieved by administration of 80 mg/kg α-chloralose, followed by continuous infusion at 28 mg/kg/hr. Arterial pH and pressures of O_2 and CO_2 were measured with a blood gas analyzer (AVL Compact 3; Diamond Diagnostics, Holliston, MA) and were adjusted by regulating the respiratory rate and volume. Body temperature was maintained at 37°C.

The experimental procedure for infusion of [3-^{13}C]lactate was first established in three rats. Glucose was continuously infused at 0.15 mmol/kg/min to avoid production of ^{13}C-enriched glucose from [3-^{13}C]lactate in peripheral tissues. Then rats received an exponential bolus of 0.5 mmol/kg of [3-^{13}C]lactate for 5 min and then a continuous infusion at 0.07 mmol/kg/min. This rate was then adjusted based on measured plasma lactate levels. A sustained plasma lactate concentration and FE were achieved by following this protocol, as confirmed in collected plasma samples.

Plasma glucose and lactate concentrations were quantified with the glucose and lactate oxidase methods, respectively, by using GM7 Micro-Stat analyzers (Analox Instruments, London, United Kingdom). FE of substrates in plasma samples was measured by MRS in vitro (Duarte et al., 2007).

MRS

All MRS experiments in vivo were carried out in a DirectDrive spectrometer (Agilent Technologies, Palo Alto, CA) interfaced with a 26-cm horizontal-bore 14.1-T magnet (Magnex Scientific, Abingdon, United Kingdom) with a home-built coil consisting of a ^1H quadrature surface coil and a ^{13}C linearly polarized surface coil, as detailed previously (Duarte et al., 2011). Briefly, the static magnetic field in the brain (volume of interest 320 μl) was homogenized by FAST(EST)MAP shimming (Gruetter and Tkáč, 2000), localized ^1H MRS was performed by using STEAM with an echo time of 2.8 msec and a repetition time of 4 sec (Mlynárik et al., 2006); ^{13}C MRS was performed with semiadiabatic distortionless enhancement by polarization transfer (DEPT) combined with 3D-ISIS ^1H localization (Henry et al., 2003a); and LCModel (Stephen Provencher, Oakville, Ontario, Canada) was employed for analysis of both ^1H (Mlynárik et al., 2006) and ^{13}C (Henry et al., 2003b) spectra.

The scaling of ^{13}C concentrations measured in vivo was based on the FE determined in vitro in ^{13}C MRS from perchloric acid extracts of the brain prepared at the end of each experiment, as described elsewhere (Duarte and Gruetter, 2013). For that, lyophilized extracts were redissolved in ^2H_2O and the p^2H was adjusted to 7.0 with ^2HCl or NaO^2H solutions. High-resolution in vitro MRS was performed as detailed by Duarte et al. (2007) with a 14.1-T DRX-600 spectrometer equipped with a 5-mm cryoprobe (Bruker BioSpin SA, Fällenden, Switzerland).

Metabolic Modeling

Labeling incorporation from [3-^{13}C]lactate into aliphatic carbons glutamate and glutamine was analyzed by using the one- and two-compartment models previously described by Henry et al. (2002) and Duarte et al. (2011), respectively

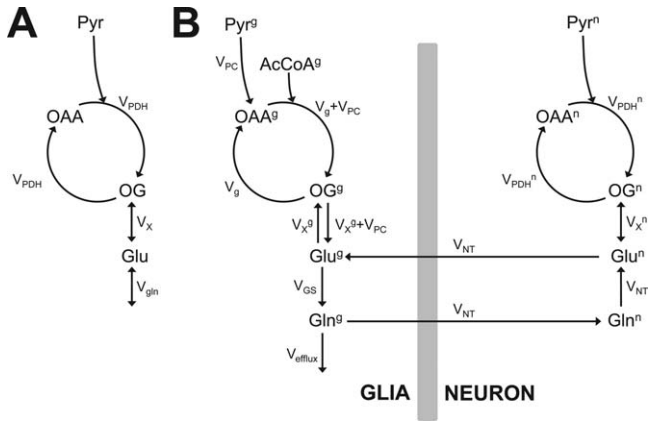

Fig. 1. Schematics of the metabolic models employed for analysis of ^{13}C enrichment curves measured in vivo by MRS. In the models of brain energy metabolism with one (**A**) and two (**B**) compartments, pyruvate (Pyr) pools are in fast equilibrium with lactate and are diluted by unlabeled substrates, namely, glucose. $V_{PDH}{}^n$ is the neuronal TCA cycle; $V_g + V_{PC}$ is the total glial TCA cycle; V_{PC} is the rate of pyruvate carboxylase. In the glial compartment, the acetyl-CoA (AcCoA) pool originates from pyruvate and can be diluted further by glia-specific substrates. TCA cycle intermediates oxaloacetate (OAA) and 2-oxoglutarate (OG) are in exchange with amino acids through V_X. The apparent glutamatergic neurotransmission (i.e., glutamate–glutamine cycle) is V_{NT}, and the glutamine synthetase rate is V_{GS} (equal to $V_{PC} + V_{NT}$). Efflux of labeling from the metabolic system occurs through the rate of glial glutamine loss V_{efflux} (equal to V_{PC}). The superscripts g and n distinguish metabolic pools or fluxes in the glial or neuronal compartment, respectively.

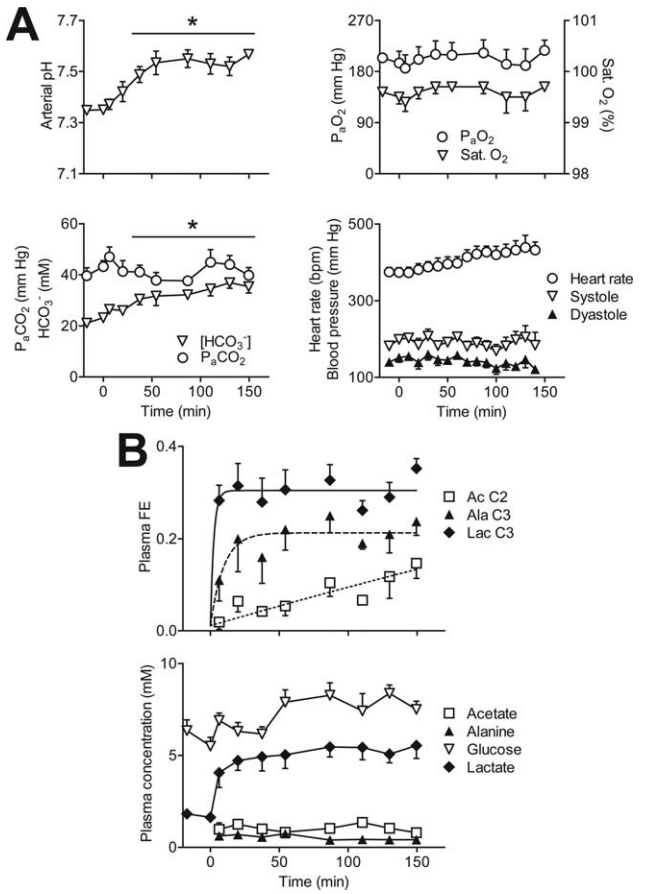

Fig. 2. Blood physiology parameters (**A**) and FE and concentration of substrates in the plasma (**B**). In A, asterisks indicate that pH and concentration of HCO^{3-} were significantly increased compared with baseline ($P < 0.05$, paired *t*-test). In B, concentration of glucose and lactate (Lac) were measured biochemically, whereas alanine (Ala) and acetate (Ac) contents as well as FE were determined in plasma samples by ^1H MRS.

(Fig. 1). The mathematical models were adjusted to the ^{13}C enrichment curves of glutamate and glutamine by nonlinear regression with the Levenberg-Marquardt algorithm, coupled to a Runge-Kutta method to obtain numerical solutions of the ordinary differential equations that define each model. The one-compartment model was fit only to curves of glutamate C3 and C4. In the analysis with the two-compartment model, accuracy was improved by constraining glial metabolic fluxes according to a previous study under identical experimental conditions in which rats were infused with [1,6-^{13}C]glucose (Duarte et al., 2011). The flux of the glial tricarboxylic acid (TCA; $V_{TCA}{}^g$) cycle was constrained to 38% of the whole mitochondrial oxidation, i.e., total pyruvate oxidation $CMR_{pyr(ox)}$; the flux through pyruvate carboxylation (V_{PC}) was defined as 25% of $V_{TCA}{}^g$; and the transmitochondrial 2-oxoglutarate/glutamate exchange flux in the glia ($V_X{}^g$) was considered equal to V_g, which denotes the fraction of flux through glial pyruvate dehydrogenase corresponding to the complete oxidation of pyruvate. In addition to metabolic fluxes, fitted parameters included the FE of glial acetyl-CoA and pyruvate in both compartments. The reliability of measured parameters was evaluated by Monte-Carlo analysis (Duarte et al., 2011). The variance of each parameter was estimated by fitting a gamma function to the probability distribution resulting from 500 Monte-Carlo simulations. All numerical procedures were performed in Matlab (The MathWorks, Natick, MA). Fitted parameters are reported with SD. Remaining results are mean ± SEM of n = 5.

RESULTS

Blood Physiology and Substrate Enrichment

To measure blood pH and gases, plasma concentrations and ^{13}C FEs of lactate, alanine, acetate, and glucose, arterial blood samples were collected periodically. Administration of lactate was accompanied by an increase of pH and bicarbonate in the arterial blood without significant effects in other measured physiological parameters (Fig. 2A). Blood pH increased from 7.35 ± 0.01 before infusion to 7.57 ± 0.01 after 3 hr (3.0% ± 0.2%), and bicarbonate increased from 21.1 ± 1.2 mM to 35.4 ± 2.5 mM (68% ± 7%) at the end of the experiment. The target plasma lactate concentration was attained after administration of the [3-^{13}C]lactate bolus, whereas the plasma levels of other potential brain substrates did not vary substantially (Fig. 2B). The current infusion protocol resulted in marked hyperlactemia and fairly constant plasma lactate C3 enrichment (0.31 ± 0.01) 5 min after starting the

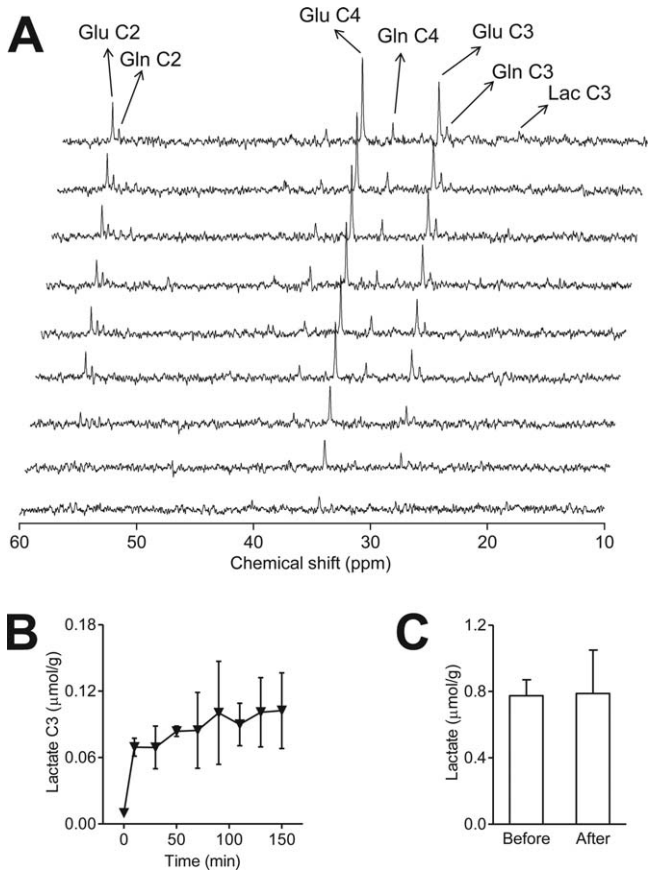

Fig. 3. **A**: Typical ^{13}C NMR spectra acquired in vivo at 14.1 T from the rat brain during infusion of [3-^{13}C]lactate. Each spectrum was acquired for 18 min, and Lorentzian-Gaussian apodization was employed with lb = 7, gf = 0.12, and gfs = 0.02. **B:** Brain lactate C3 content increased upon infusion of [3-^{13}C]lactate, but its quantification was associated with relatively high uncertainty. **C:** Initial concentration of lactate was quantified by ^{1}H MRS in vivo before the ^{13}C MRS experiment, and brain lactate content at the end was estimated from the last data point of the labeling curve and the FE measure in brain extracts. Data are shown as mean ± SEM for five rats.

administration of [3-^{13}C]lactate. Labeling was also observed in plasma alanine C3 and acetate C2 but not glucose C1. Whereas FE of alanine reached a plateau at 0.21 ± 0.02, that of acetate increased continuously throughout the experiment (0.15 ± 0.03 at the end).

Brain ^{13}C-Enriched Metabolites

Initial total brain lactate content measured by ^{1}H MRS prior to infusion was 0.77 ± 0.10 μmol/g. The singlet resonance of lactate C3 was observed upon [3-^{13}C]lactate infusion (Fig. 3A) and allowed estimating its concentration over time (Fig. 3B). In brain extracts performed at the end of the MRS experiments, FE of lactate C3 was 0.13 ± 0.02, which was not significantly different from that of alanine C3 (0.10 ± 0.01, $P > 0.05$, paired *t*-test). Labeling of brain glucose and acetate was undetectable both in vivo and in brain extracts. Brain lactate C3 concentration measured in vivo and its enrichment measured in tissue extracts were used to estimate total brain lactate content, which was similar to that measured before [3-^{13}C]lactate infusion (Fig. 3C).

TABLE I. FE of Glutamate and Glutamine Measured in Perchloric Acid Extracts of the Brains From the Experiments In Vivo

	Glutamate	Glutamine
C4	0.115 ± 0.009	0.078 ± 0.014
C3	0.101 ± 0.014	0.072 ± 0.022
C2	0.108 ± 0.016	0.068 ± 0.014

Labeling from [3-^{13}C]lactate into aliphatic carbons of brain glutamate and glutamine was measured in the rat brain with a time resolution of 18 min (Fig. 3A). Other neurochemicals, such as γ-aminobutyric acid (GABA) and aspartate, became enriched but were not reliably quantified at this temporal resolution (not shown). The ^{13}C enrichment of glutamate and glutamine was quantified in brain extracts (Table I) and then used to scale the experimental curves obtained in vivo for metabolic modeling (Fig. 4). The concentration of amino acids was assumed to remain unaltered through the whole period of lactate infusion.

Estimation of Metabolic Fluxes

To determine the metabolic fluxes, the one- and two-compartment models depicted in Figure 1 (for details see Henry et al., 2002; Duarte et al., 2011) were fitted to the average enrichment in aliphatic carbons of glutamate and glutamine (Fig. 4A). The estimated metabolic fluxes were similar to those previously determined upon infusion of [1,6-^{13}C]glucose (Fig. 4B). Namely, the neuronal TCA cycle (V_{PDH}^{n}) was 0.40 ± 0.02 μmol/g/min, the mitochondrial exchange (V_X^{n}) was 0.68 ± 0.33 μmol/g/min, and the glutamate–glutamine cycle (V_{NT}) was 0.14 ± 0.05 μmol/g/min. Fluxes in the glial compartment were constrained based on the relative rates measured upon administration of [1,6-^{13}C]glucose (Duarte et al., 2011) as detailed in Materials and Methods. This resulted in $V_{PC} = 0.072 \pm 0.004$ μmol/g/min and $V_g = V_X^{g} = 0.22 \pm 0.01$ μmol/g/min. FE of neuronal pyruvate C3 was 0.13 ± 0.01. In the glial compartment, FE was 0.062 ± 0.013 for pyruvate C3 and 0.049 ± 0.013 for acetyl-CoA C2. Constraining the enrichment of these two precursors in the glial compartment to be equal resulted in identical fit quality and flux values (not shown). Based on the plasma FE of 0.31 (Fig. 2B), one can estimate that plasma lactate contributed to 43% of neuronal pyruvate and to 20% and 17% of glial pyruvate and acetyl-CoA, respectively.

To estimate the variability of measured fluxes across experiments, the two-compartment model was also fitted to ^{13}C enrichment curves from each animal. The fit of individual data sets resulted in mean metabolic fluxes similar to those determined from the average curves but associated with larger standard deviations representing both

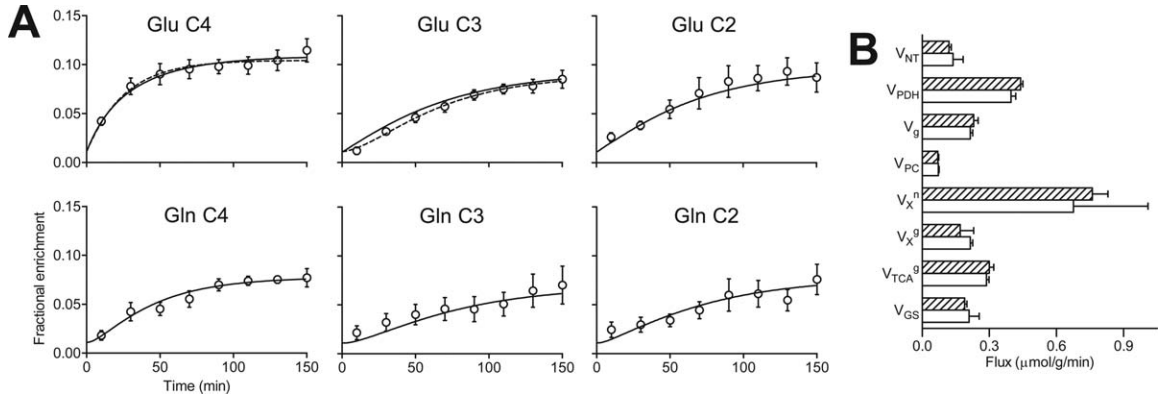

Fig. 4. FE in carbons of glutamate (Glu) and glutamine (Gln) measured in vivo by ^{13}C MRS (**A**) and resulting metabolic fluxes (**B**). In A, curves of the best fit of the one- and two-compartment models are represented by dashed and solid lines, respectively. Data are shown as mean ± SEM for five rats. B shows the metabolic fluxes obtained by fitting the two-compartment model to ^{13}C enrichment curves of glutamate and glutamine from experiments with administration of [3-^{13}C]lactate (open bars) or [1,6-^{13}C]glucose (haycheded bars; data from Duarte et al., 2011). Error bars of fluxes are SD.

experimental and biological variability. In particular, the freely fitted fluxes V_{PDH}^n, V_X^n, and V_{NT} were 0.33 ± 0.14, 23 ± 51, and 0.24 ± 0.26 μmol/g/min, respectively. The constrained glial fluxes V_{PC} and V_g (= V_X^g) were 0.059 ± 0.026 and 0.18 ± 0.08 μmol/g/min, respectively.

Given the number of constraints imposed on the model, we tested the result of fitting the simple one-compartment model to the curves of glutamate C3 and C4 further. The fit of the one-compartment model resulted in V_{PDH} and V_X of 0.33 ± 0.02 and 3.0 ± 116.0 μmol/g/min, respectively. The dilution of glutamate by unlabeled glutamine (V_{gln}) was 0.033 ± 0.009 μmol/g/min, and the FE of pyruvate C3 was 0.12 ± 0.01. These parameters were indistinct from those measured with the two-compartment model (Fig. 4B) and remained unaltered (V_{PDH} = 0.33 ± 0.01 μmol/g/min, V_{gln} = 0.031 ± 0.008 μmol/g/min) when V_X was fixed to 5 μmol/g/min, a value that is one order of magnitude higher than the TCA cycle rates determined with the two-compartment model (Henry et al., 2002).

Effect of Model Assumptions on Flux Estimation

In the current study, the fluxes in the glial compartment could not be accurately estimated without imposing constraints on the mathematical model. It was assumed that V_{PC} was 25% of V_{TCA}^g. Smaller V_{PC} values had little effect on the estimated parameters, but a relative increase affected mostly V_{NT} and V_X^n (Fig. 5A). For example, the increase of V_{PC}/V_{TCA}^g by 20% resulted in an increase of V_{PC} (24%) and V_{NT} (40%) and a reduction of V_X^n (28%). It should be noted that lower V_{PC} relative to V_{TCA}^g led to poorer estimation of V_X^n. The lowest sum of squared residuals (SSR) was obtained with V_{PC} at 20% of V_{TCA}^g.

V_{TCA}^g was constrained to 38% of the total pyruvate oxidation, $CMR_{pyr(ox)}$. A modification in the ratio of V_{TCA}^g to $CMR_{pyr(ox)}$ resulted in prominent alterations not only in glial but also in neuronal fluxes (Fig. 5B). The relative increase in V_{TCA}^g was, as expected, associated with diminished neuronal oxidative metabolism, depicted by V_{PDH}^n. V_{NT} was modified principally when the fraction of glial oxidative metabolism was increased. For example, when considering that V_{TCA}^g was 46% of $CMR_{pyr(ox)}$, V_{NT} was 0.19 ± 0.06 μmol/g/min; i.e., it was overestimated by 37%. Both increase and decrease of the fraction of V_{TCA}^g led to an increase of SSR, i.e., reduction of fit quality.

The assumption in the value of the glial transmitochondrial exchange flux V_X^g was virtually devoid of effects in the parameters estimated by the mathematical model (Fig. 5C). Similarly, varying the relative concentrations of glutamate and glutamine and their distribution within the glial and neuronal compartments did not cause major alterations to the estimated fluxes (Fig. 6). An increase in the relative size of the glial pool of glutamate was, however, associated with poorer fitting, i.e., a large increase in SSR.

DISCUSSION

The current article describes the metabolic fluxes of brain energy metabolism in the rat brain in vivo, measured with ^{13}C-enriched lactate as tracer. Although lactate is transported across the blood–brain barrier with a permeability about half of that of glucose (Knudsen et al., 1991), this study shows that, upon administration of [3-^{13}C]lactate, ^{13}C MRS can be used to study energy metabolism in the rodent brain under normoglycemic conditions. Metabolic fluxes determined with [3-^{13}C]lactate were similar to those estimated with other tracers, namely, isotopes of glucose under identical experimental conditions (for review see Lanz et al., 2013).

Lactate Transport and Utilization

Although lactate C3 peaks were identifiable by ^{13}C MRS in vivo, the quantification was not sufficiently reliable to estimate lactate uptake from blood. Nevertheless, lactate concentration was 0.77 μmol/g in the rat brain

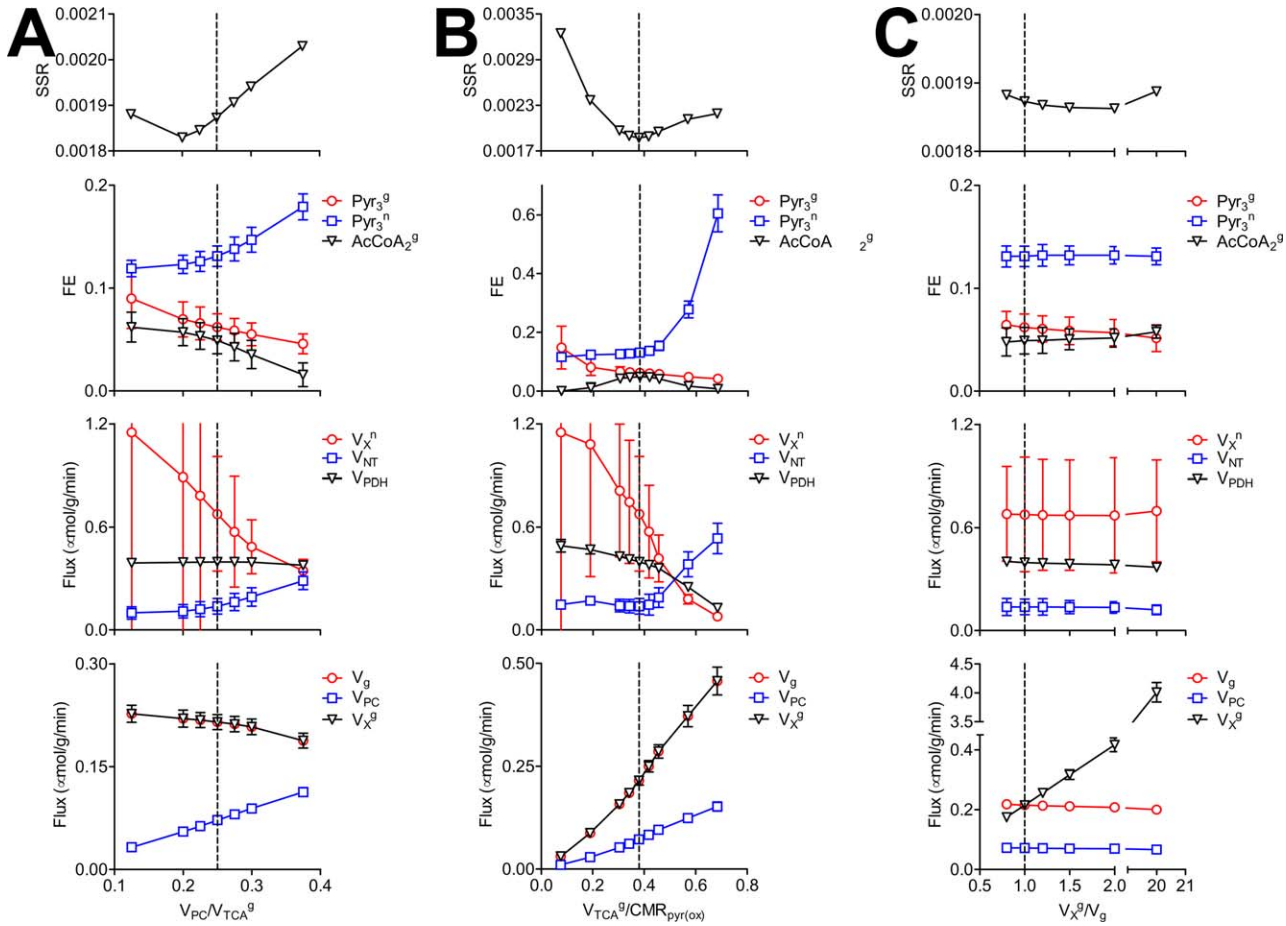

Fig. 5. Effect of the constraints imposed to V_{PC} (**A**), $V_{TCA}{}^{g}$ (**B**), and $V_X{}^{g}$ (**C**) on parameter estimation with the two-compartment model. Vertical dashed lines represent the assumptions used for parameter estimation. Error bars are SD. [Color figure can be viewed in the online issue, which is available at wileyonlinelibrary.com.]

under α-chloralose before [3-^{13}C]lactate infusion and was not augmented markedly upon infusion. At the end of the experiment, brain lactate enrichment was only 13% in C3.

The mechanism by which lactate crosses the human blood–brain barrier is equilibrative (Knudsen et al., 1991). Lactate influx into the rat brain consists of a saturable, stereospecific component to the L-enantiomer with transport rate constants that are approximately 50% of those for glucose and a nonsaturable, nonstereospecific diffusion component that has been determined from D-lactate influx (Lear and Kasliwal, 1991; LaManna et al., 1993). A ^{13}C MRS study in humans confirmed that, indeed, brain lactate uptake and metabolism increase with plasma lactate concentration (Boumezbeur et al., 2010). From this study, it can be estimated that the maximum contribution of plasma lactate to the whole-brain oxidative metabolism is 2–3% at physiological plasma lactate levels (1–1.5 mM) and can reach 60% at supraphysiological plasma lactate levels, i.e., when carriers are nearly saturated. Furthermore, ^{13}C enrichment patterns in glutamate and glutamine indicate that lactate metabolism in the brain is similar to that of glucose (Boumezbeur et al., 2010). This was reproduced in the current study, in which blood lactate at supraphysiological levels contributed to 43% of neuronal pyruvate in the rat brain. In contrast, glial pyruvate received a contribution of plasma lactate of only 20%. However, the exact value of lactate utilization was not directly estimated in the current study. The cerebral metabolic rate of lactate (CMR_{lac}) increases with increasing lactemia (Gallagher et al., 2009; Boumezbeur et al., 2010; Rasmussen et al., 2010; van Hall, 2010). Lactate transport was evaluated in several regions of the rat brain by LaManna et al. (1993). By using the mean kinetic parameters described in this study, excluding those for cerebellum, transport into and out of the brain was 0.27 and 0.07 μmol/g/min at our lactate concentrations. At steady state, CMR_{lac} is thus 0.20 μmol/g/min. By subtracting CMR_{lac} from the whole pyruvate oxidation, glucose utilization (CMR_{glc}) was 28 μmol/g/min. Although this rate of glucose oxidation is much smaller than what had been determined under the same experimental conditions but normolactemia (Duarte et al., 2011; Duarte and Gruetter, 2012, 2013), it is well known that increases in

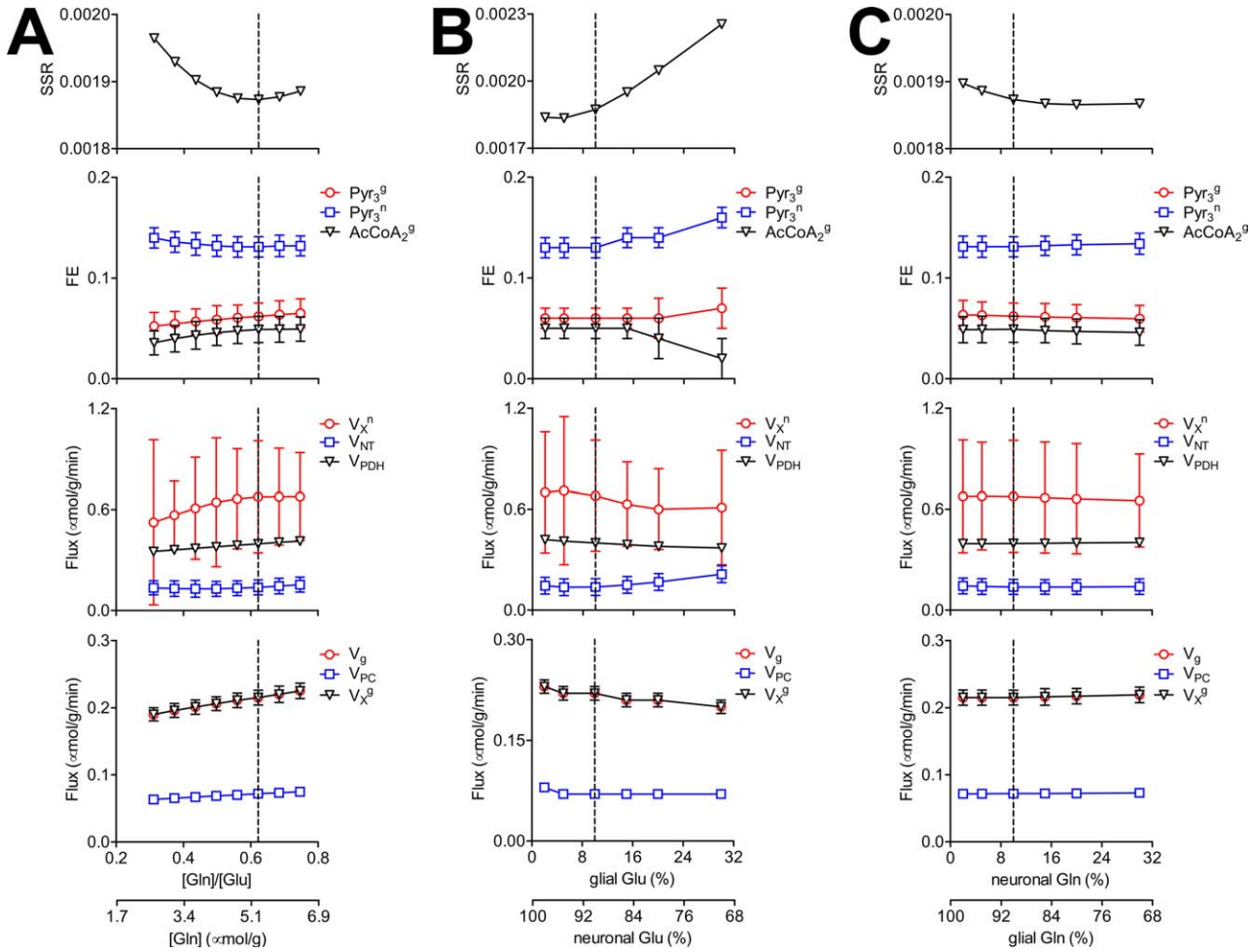

Fig. 6. Relative size of glutamate and glutamine pools has little effect on the estimated parameters with the two-compartment model. **A:** Effect of total glutamine concentration while glutamate remained unvaried. **B,C:** Effect of the relative distribution of glutamate and glutamine in each compartment, respectively. Vertical dashed lines represent the assumptions used for parameter estimation. Error bars are SD. [Color figure can be viewed in the online issue, which is available at wileyonlinelibrary.com.]

lactate uptake and oxidation are paralleled by glycolysis inhibition (Hertz et al., 2014).

Transport of lactate is pH dependent (Oldendorf et al., 1979; Knudsen et al., 1991), and hyperlactemia raises blood pH, as observed by others (Leegsma-Vogt et al., 2003; Smith et al., 2003). Nevertheless, variable contribution of lactate consumption was not considered for the modeling of brain energy metabolism. Although lactate transport kinetics were not measured in the current study, at supraphysiological levels of plasma lactate the variation of pH in 0.2 units is unlikely to affect its cerebral metabolic rate. From the data published by Oldendorf et al. (1979) on Wistar rats under pentobarbital anesthesia and normolactemia, the increase in pH observed in the current study would result in a reduction of lactate uptake by only 8%, which is within the standard deviation of measured lactate uptake.

Energy Metabolism in Neurons and Glia

Infusion of unlabeled glucose prevented labeling from appearing in the positions C1 and C6 as a result of [3-^{13}C]lactate recycling through liver gluconeogenesis (Sampol et al., 2013; see also Bouzier et al., 2000; Boumezbeur et al., 2010). Indeed, glucose labeling was undetectable either in vivo or in brain extracts, ensuring that the ^{13}C enrichment observed in amino acids was derived mainly from [3-^{13}C]lactate. The current mathematical models did not include ^{13}C incorporation from alanine or acetate that became enriched in plasma. Given the low concentration of alanine relative to lactate in the blood (6- to 13-fold lower; Fig. 2B) and its relatively low transport rate, blood-borne ^{13}C-enriched alanine is unlikely to contribute significantly to brain metabolism (Duarte et al., 2011). Thus, the amount of [3-^{13}C]alanine measured in the brain probably resulted from brain metabolism of

[3-^{13}C]lactate. Plasma acetate content was also four- to sevenfold lower than lactate content, and, moreover, [2-^{13}C]acetate was undetectable in the brain. Nevertheless, the model allowed for different FE in pyruvate and acetyl-CoA, representing glial acetate utilization. In glia, the estimated FE was similar for acetyl-CoA and pyruvate (in the two-compartment model), suggesting minor utilization of acetate that would dilute the pool of acetyl-CoA relative to that of pyruvate.

In the current experiments, plasma lactate at supraphysiological levels (~5 mM) contributed to 43% and 20% of neuronal and glial oxidative metabolism, respectively. Blood-born [3-^{13}C]lactate was thus more diluted in astrocytes than in neurons, leading to pyruvate enrichment of 6% and 13%, respectively, which suggests preferential utilization of unlabeled substrates, such as glucose and glycogen, within the glial compartment. Indeed, glial glycogen is essential for the maintenance of the homeostasis of extracellular depolarizing agents such as glutamate and potassium (Sickmann et al., 2009; Xu et al., 2013) and constitutes an important precursor for the de novo synthesis of glutamate and glutamine (Gibbs et al., 2007). Given the role of astrocytes in substrate uptake from the blood stream and delivery to neurons, the current data are consistent with the presence of at least two distinct lactate pools in astrocytes, one being used to support neurons and not prone to glial oxidation. Astrocytes have been suggested to consume, eventually, as much lactate as neurons or even more (Zielke et al., 2007; Gandhi et al., 2009). In this case, the current results indicate that this lactate is not of peripheral origin but probably is locally produced. Moreover, it has been proposed that the rat brain comprises one pool of lactate that exchanges with plasma lactate "that can be filled and emptied in accordance to blood lactate concentration" and that is not used as an energy supply (Leegsma-Vogt et al., 2003). This is also compatible with subcellular compartmentation of glucose and lactate metabolism; i.e., lactate production and oxidation of exogenous lactate are functionally separate metabolic pathways. This has been proposed to occur in astrocytes (Brand et al., 1992) and neurons (Cruz et al., 2001) or in peripheral organs, such as the heart (Chatham et al., 2001).

Because of the small enrichment of amino acids, particularly glutamine that was at most 8%, corresponding to nearly 0.4 μmol/g in comparison to the experiment with ^{13}C-enriched glucose administration (Duarte et al., 2011; Duarte and Gruetter, 2013), a possible difference in C2 and C3 enrichment curves was not clearly identified. Thus, the flux through pyruvate carboxylase could not be determined accurately in vivo. Therefore, the FE was determined in the brain extracts at the end of the experiment in vivo for glutamine C2 and C3 and found to be similar (Table I), which further suggests that lactate is metabolized mainly in the neuronal compartment deprived of pyruvate carboxylase activity (Bouzier et al., 2000; Sampol et al., 2013).

In the current experiments, the use of [3-^{13}C]lactate did not allow accurate determination of metabolic fluxes in glia. Given the relatively small FE observed in brain amino acids, mathematical constraints were imposed on the model. Namely, $V_{TCA}{}^{g}$, V_{PC}, and $V_X{}^{g}$ were fixed relative to the whole oxidation rate of the brain and among each other. The relative values of these fluxes were based on the findings in experiments with [1,6-^{13}C]glucose that produces high FE in brain metabolites and thus leads to high sensitivity in MRS. Nevertheless, variation of these constraints within reasonable limits had minor effects on modeling results.

The data were further analyzed with a one-compartment model fitted only to the experimental curves of glutamate C3 and C4, which are least affected by experimental noise (see Fig. 3). Although it does not provide any information on the metabolic compartmentation, this analysis does not require flux constraining, which may be advantageous for flux estimation. Because glutamate resides mostly in neurons, one can assume that the estimated V_{PDH} is a close representation of $V_{PDH}{}^{n}$. Whereas the two models rendered similar precision in the estimation of V_{PDH} (SD 5–6%) and FE of Pyr_3 (SD 8%) in neurons, the fitting with the two-compartment model resulted in larger V_{PDH}. From the FE of Pyr_3 in the one-compartment model, one can estimate that brain pyruvate received a contribution of 39% from plasma lactate, which is not substantially different from the contribution to $Pyr_3{}^{n}$ of 43% determined by using two compartments.

The signal-to-noise ratio achieved in the current experiments was much lower than that in experiments under identical conditions but with infusion of ^{13}C-enriched glucose (Duarte et al., 2011; Duarte and Gruetter, 2013) because the observed metabolites were fivefold less enriched. This limited the analysis to the most concentrated amino acids, glutamate and glutamine, and restricted the temporal resolution to 18 min. Only glutamate C4 could be reliably quantified at a higher temporal resolution. Metabolic modeling including glutamate C4 with a resolution of ~10 min did not affect the estimation of metabolic fluxes substantially (not shown).

Although rates of oxidative metabolism were similar to those measured with ^{13}C-glucose, the utilization of lactate might be associated with a reduction in glucose metabolic rate (Smith et al., 2003). Nevertheless, the results from this study do not exclude that hyperlactemia might affect metabolic interactions between the cellular compartments. We conclude that extracerebral lactate can be used as fuel by the brain under normoglycemic conditions, leading mostly to production of pyruvate for neuronal oxidation.

ACKNOWLEDGMENTS

The authors have no conflicts of interest.

REFERENCES

Bergersen LH, Gjedde A. 2012. Is lactate a volume transmitter of metabolic states of the brain? Front Neuroenergetics 4:5.

Berthet C, Lei H, Thevenet J, Gruetter R, Magistretti PJ, Hirt L. 2009. Neuroprotective role of lactate after cerebral ischemia. J Cereb Blood Flow Metab 29:1780–1789.

Boumezbeur F, Petersen KF, Cline GW, Mason GF, Behar KL, Shulman GI, Rothman DL. 2010. The contribution of blood lactate to brain energy metabolism in humans measured by dynamic ^{13}C nuclear magnetic resonance spectroscopy. J Neurosci 30:13983–13991.

Bouzier AK, Thiaudiere E, Biran M, Rouland R, Canioni P, Merle M. 2000. The metabolism of [3-^{13}C]lactate in the rat brain is specific of a pyruvate carboxylase-deprived compartment. J Neurochem 75: 480–486.

Brand A, Engelmann J, Leibfritz D. 1992. A ^{13}C NMR study on fluxes into the TCA cycle of neuronal and glial tumor cell lines and primary cells. Biochimie 74:941–948.

Brooks. 2009. Cell–cell and intracellular lactate shuttles. J Physiol 587: 5591–5600.

Chatham JC, Des Rosiers C, Forder JR. 2001. Evidence of separate pathways for lactate uptake and release by the perfused rat heart. Am J Physiol Endocrinol Metab 281:E794–E802.

Cruz F, Villalba M, García-Espinosa MA, Ballesteros P, Bogónez E, Satrústegui J, Cerdán S. 2001. Intracellular compartmentation of pyruvate in primary cultures of cortical neurons as detected by ^{13}C NMR spectroscopy with multiple ^{13}C labels. J Neurosci Res 66:771–781.

Cureton EL, Kwan RO, Dozier KC, Sadjadi J, Pal JD, Victorino GP. 2010. A different view of lactate in trauma patients: protecting the injured brain. J Surg Res 159:468–473.

Dienel GA. 2012a. Fueling and imaging brain activation. ASN Neuro 4: e00093. doi:10.1042/AN20120021.

Dienel GA. 2012b. Brain lactate metabolism: the discoveries and the controversies. J Cereb Blood Flow Metab 32:1107–1138.

Duarte JMN, Gruetter R. 2012. Characterization of cerebral glucose dynamics in vivo with a four-state conformational model of transport at the blood–brain barrier. J Neurochem 121:396–406.

Duarte JMN, Gruetter R. 2013. Glutamatergic and GABAergic energy metabolism measured in the rat brain by ^{13}C NMR spectroscopy at 14.1 T. J Neurochem 126:579–590.

Duarte JMN, Cunha RA, Carvalho RA. 2007. Different metabolism of glutamatergic and GABAergic compartments in superfused hippocampal slices characterized by nuclear magnetic resonance spectroscopy. Neuroscience 144:1305–1313.

Duarte JMN, Carvalho RA, Cunha RA, Gruetter R. 2009. Caffeine consumption attenuates neurochemical modifications in the hippocampus of streptozotocin-induced diabetic rats. J Neurochem 111: 368–379.

Duarte JMN, Lanz B, Gruetter R. 2011. Compartmentalized cerebral metabolism of [1,6-^{13}C]glucose determined by in vivo ^{13}C NMR spectroscopy at 14.1 T. Front Neuroenergetics 3:3.

Gallagher CN, Carpenter KL, Grice P, Howe DJ, Mason A, Timofeev I, Menon DK, Kirkpatrick PJ, Pickard JD, Sutherland GR, Hutchinson PJ. 2009. The human brain utilizes lactate via the tricarboxylic acid cycle: a ^{13}C-labelled microdialysis and high-resolution nuclear magnetic resonance study. Brain 132:2839–2849.

Gandhi GK, Cruz NF, Ball KK, Dienel GA. 2009. Astrocytes are poised for lactate trafficking and release from activated brain and for supply of glucose to neurons. J Neurochem 111:522–536.

Gibbs ME, Lloyd HG, Santa T, Hertz L. 2007. Glycogen is a preferred glutamate precursor during learning in 1-day-old chick: biochemical and behavioral evidence. J Neurosci Res 85:3326–3333.

Gordon GR, Choi HB, Rungta RL, Ellis-Davies GC, MacVicar BA. 2008. Brain metabolism dictates the polarity of astrocyte control over arterioles. Nature 456:745–749.

Gruetter R, Tkác I. 2000. Field mapping without reference scan using asymmetric echo-planar techniques. Magn Reson Med 43:319–323.

Henry PG, Lebon V, Vaufrey F, Brouillet E, Hantraye P, Bloch G. 2002. Decreased TCA cycle rate in the rat brain after acute 3-NP treatment measured by in vivo ^{1}H-[^{13}C]NMR spectroscopy. J Neurochem 82:857–866.

Henry PG, Tkác I, Gruetter R. 2003a. ^{1}H-localized broadband ^{13}C NMR spectroscopy of the rat brain in vivo at 9.4 T. Magn Reson Med 50:684–692.

Henry PG, Oz G, Provencher S, Gruetter R. 2003b. Toward dynamic isotopomer analysis in the rat brain in vivo: automatic quantitation of ^{13}C NMR spectra using LCModel. NMR Biomed 16:400–412.

Hertz L. 2012. Metabolic studies in brain slices: past, present, and future. Front Pharmacol 3:26.

Hertz L, Gibbs ME, Dienel GA. 2014. Fluxes of lactate into, from, and among gap junction-coupled astrocytes and their interaction with noradrenaline. Front Neurosci 8:261.

Jeffrey FM, Marin-Valencia I, Good LB, Shestov AA, Henry PG, Pascual JM, Malloy CR. 2013. Modeling of brain metabolism and pyruvate compartmentation using ^{13}C NMR in vivo: caution required. J Cereb Blood Flow Metab 33:1160–1167.

Knudsen GM, Paulson OB, Hertz MM. 1991. Kinetic analysis of the human blood–brain barrier transport of lactate and its influence by hypercapnia. J Cereb Blood Flow Metab 11:581–586.

LaManna JC, Harrington JF, Vendel LM, Abi-Saleh K, Lust WD, Harik SI. 1993. Regional blood–brain lactate influx. Brain Res 614: 164–170.

Lanz B, Gruetter R, Duarte JMN. 2013. Metabolic flux and compartmentation analysis in the brain in vivo. Front Endocrinol 4: 156.

Lauritzen KH, Morland C, Puchades M, Holm-Hansen S, Hagelin EM, Lauritzen F, Attramadal H, Storm-Mathisen J, Gjedde A, Bergersen LH. 2014. Lactate receptor sites link neurotransmission, neurovascular coupling, and brain energy metabolism. Cereb Cortex 24:2784–95.

Lear JL, Kasliwal RK. 1991. Autoradiographic measurement of cerebral lactate transport rate constants in normal and activated conditions. J Cereb Blood Flow Metab 11:576–580.

Lee Y, Morrison BM, Li Y, Lengacher S, Farah MH, Hoffman PN, Liu Y, Tsingalia A, Jin L, Zhang PW, Pellerin L, Magistretti PJ, Rothstein JD. 2012. Oligodendroglia metabolically support axons and contribute to neurodegeneration. Nature 487:443–448.

Leegsma-Vogt G, Venema K, Korf J. 2003. Evidence for a lactate pool in the rat brain that is not used as an energy supply under normoglycemic conditions. J Cereb Blood Flow Metab 23:933–941.

Mlynárik V, Gambarota G, Frenkel H, Gruetter R. 2006. Localized short-echo-time proton MR spectroscopy with full signal-intensity acquisition. Magn Reson Med 56:965–970.

Newman LA, Korol DL, Gold PE. 2011. Lactate produced by glycogenolysis in astrocytes regulates memory processing. PLoS One 6:e28427.

Oldendorf W, Braun L, Cornford E. 1979. pH dependence of blood–brain barrier permeability to lactate and nicotine. Stroke 10:577–581.

Pellerin L, Magistretti PJ. 1994. Glutamate uptake into astrocytes stimulates aerobic glycolysis: a mechanism coupling neuronal activity to glucose utilization. Proc Natl Acad Sci U S A 91:10625–10629.

Rasmussen P, Nielsen J, Overgaard M, Krogh-Madsen R, Gjedde A, Secher NH, Petersen NC. 2010. Reduced muscle activation during exercise related to brain oxygenation and metabolism in humans. J Physiol 588:1985–1995.

Rinholm JE, Hamilton NB, Kessaris N, Richardson WD, Bergersen LH, Attwell D. 2011. Regulation of oligodendrocyte development and myelination by glucose and lactate. J Neurosci 31:538–548.

Ros J, Pecinska N, Alessandri B, Landolt H, Fillenz M. 2001. Lactate reduces glutamate-induced neurotoxicity in rat cortex. J Neurosci Res 66:790–794.

Sampol D, Ostrofet E, Jobin ML, Raffard G, Sanchez S, Bouchaud V, Franconi JM, Bonvento G, Bouzier-Sore AK. 2013. Glucose and lactate metabolism in the awake and stimulated rat: a ^{13}C-NMR study. Front Neuroenergetics 5:5.

Schurr A, Payne RS, Miller JJ, Rigor BM. 1997. Brain lactate is an obligatory aerobic energy substrate for functional recovery after hypoxia: further in vitro validation. J Neurochem 69:423–426.

Schurr A, Miller JJ, Payne RS, Rigor BM. 1999. An increase in lactate output by brain tissue serves to meet the energy needs of glutamate-activated neurons. J Neurosci 19:34–39.

Schurr A, Payne RS, Miller JJ, Tseng MT, Rigor BM. 2001. Blockade of lactate transport exacerbates delayed neuronal damage in a rat model of cerebral ischemia. Brain Res 895:268–272.

Sickmann HM, Walls AB, Schousboe A, Bouman SD, Waagepetersen HS. 2009. Functional significance of brain glycogen in sustaining glutamatergic neurotransmission. J Neurochem 109(Suppl 1):80–86.

Smith D, Pernet A, Hallett WA, Bingham E, Marsden PK, Amiel SA. 2003. Lactate: a preferred fuel for human brain metabolism in vivo. J Cereb Blood Flow Metab 23:658–664.

Suzuki A, Stern SA, Bozdagi O, Huntley GW, Walker RH, Magistretti PJ, Alberini CM. 2011. Astrocyte–neuron lactate transport is required for long-term memory formation. Cell 144:810–823.

van Hall G. 2010. Lactate kinetics in human tissues at rest and during exercise. Acta Physiol 199:499–508.

Wender R, Brown AM, Fern R, Swanson RA, Farrell K, Ransom BR. 2000. Astrocytic glycogen influences axon function and survival during glucose deprivation in central white matter. J Neurosci 20:6804–6810.

Xu J, Song D, Xue Z, Gu L, Hertz L, Peng L. 2013. Requirement of glycogenolysis for uptake of increased extracellular K^+ in astrocytes: potential implications for K^+ homeostasis and glycogen usage in brain. Neurochem Res 38:472–485.

Zielke HR, Zielke CL, Baab PJ, Tildon JT. 2007. Effect of fluorocitrate on cerebral oxidation of lactate and glucose in freely moving rats. J Neurochem 101:9–16.